A FORMATION TIMESCALE OF THE GALACTIC HALO FROM MG ISOTOPES IN DWARF STARS*

Marília Carlos,[1,2] Amanda I. Karakas,[2] Judith G. Cohen,[3] Chiaki Kobayashi,[4] and Jorge Meléndez[1]

[1] *Universidade de São Paulo, IAG, Departamento de Astronomia*

Rua do Matão 1226, Cidade Universitária, 05508-900, São Paulo, SP, Brazil

[2] *Monash Centre for Astrophysics, School of Physics and Astronomy, Monash University*

Victoria 3800, Australia

[3] *California Institute of Technology*

1200 E. California Boulevard, MC 249-17, Pasadena, CA 91195, USA

[4] *Centre for Astrophysics Research, School of Physics, Astronomy and Mathematics, University of Hertfordshire*

College Lane, Hatfield AL10 9AB, UK

ABSTRACT

We determine magnesium isotopic abundances of metal poor dwarf stars from the galactic halo, to shed light on the onset of asymptotic giant branch (AGB) star nucleossynthesis in the galactic halo and constrain the timescale of its formation. We observed a sample of eight new halo K dwarfs in a metallicity range of $-1.9 <$ [Fe/H] < -0.9 and $4200 < T_{\rm eff}({\rm K}) < 4950$, using the HIRES spectrograph at the Keck Observatory ($R \approx 10^5$ and $200 \leq {\rm S/N} \leq 300$). We obtain magnesium isotopic abundances by spectral synthesis on three MgH features and compare our results with galactic chemical evolution models. With the current sample, we almost double the number of metal poor stars with Mg isotopes determined from the literature. The new data allow us to determine the metallicity when the ^{26}Mg abundances start to became important, [Fe/H] $\sim -1.4 \pm 0.1$. The data with [Fe/H] > -1.4 are somewhat higher (1-3 σ) than previous chemical evolution model predictions, indicating perhaps higher yields of the neutron-rich isotopes. Our results using only AGB star enrichment suggest a timescale for formation for the galactic halo of about 0.3 Gyr, but considering also supernova enrichment, the upper limit for the timescale formation is about 1.5 Gyr.

Keywords: Galaxy: halo – stars: abundances – stars: AGB and post-AGB

Corresponding author: Marília Carlos
marilia.carlos@usp.br

1. INTRODUCTION

The study of galaxy formation and evolution is a vigorous field of astronomy, with many studies in the literature debating how our Galaxy evolved dynamically and chemically. Regarding the studies of the evolution of the Galactic halo, an important uncertainty is its formation timescale. The classic work of Eggen et al. (1962) discusses a monolithic scenario in which a fast dissipative collapse occurs on a timescale of 200 million years. Later, Searle & Zinn (1978) suggested a central collapse, but implied that the outer halo was formed by the merging of larger fragments, resulting in a formation timescale > 1 Gyr. The latter approach is similar to current cosmological ΛCDM models in which larger galaxies, such as the Milk Way, were formed hierarchically (e.g., Navarro et al. 1997 and Zolotov et al. 2009). Hierarchical chemico-dynamical models show that 80% of the galactic halo has [O/Fe]$\gtrsim 0.5$ (Kobayashi & Nakasato 2011, Figure 9) and Tissera et al. (2012) indicate the presence of accreted stars with high $\alpha-$enhancement in the outer region of the galactic halo. Those hierarchical models are in agreement with observations that indicate that there are at least two different stellar populations in the halo (e.g., Carollo et al. 2007; Nissen & Schuster 2010).

Assuming different gas infall episodes that contribute to the formation of the galactic components, chemical evolution models for the Galaxy, such as those by Chiappini et al. (1997) and Micali et al. (2013), put a constraint on the timescales of star formation and chemical enrichment of the components. These types of models find values for the formation timescale of the halo that vary from 0.2 to 2 Gyr, where the gas accretion rate depends on the formation timescale of the halo, and thin and thick disk components, which will set the metallicity distribution function of the galaxy. Thus, knowing the timescale for formation of the various components of the Galaxy can constrain chemical evolution models.

Elemental and isotopic abundances from different nucleosynthetic sites are an extremely useful tool to solve this problem. Since the different isotopes could be formed in stars of different masses, which die at different ages, they could function as "clocks" to trace the timescales of halo formation.

Magnesium in particular is a good clock because its different isotopes are produced in different sites (i.e., different stars); therefore, they trace stellar (and Galactic) evolution over short and long timescales. The element magnesium has three stable isotopes: ^{24}Mg, ^{25}Mg and ^{26}Mg. The magnesium isotopes ^{24,25,26}Mg are produced inside massive stars, while the isotopes ^{25,26}Mg are also produced in stars with intermediate mass (we discuss the details of Mg production in Sect. 2). Since the ^{25,26}Mg isotopes can be produced in asymptotic giant branch (AGB) stars (Karakas & Lattanzio 2003; Fishlock et al. 2014), measuring the Mg isotopic ratios can inform us when the heavier Mg isotopes from AGB stars begin to contribute toward galactic chemical enrichment, meaning that the isotopic ratios ^{25,26}Mg/^{24}Mg increase with the onset of AGB stars.

Some chemical evolution models include the chemical abundances of magnesium and its stable isotopes (e. g. Alibés et al. 2001; Fenner et al. 2003 and Kobayashi et al. 2011). Despite the existence of these models, there are few observations and analysis of these isotopes that could indicate which model is more appropriate. It is also important to stress that isotopic abundances offer more observational links than elemental abundances, because several specific nucleosynthetic processes produce isotopes, while the elemental abundance is the sum of all the isotopes that compose an element.

There are several important contributions in the literature regarding the determination of Mg isotopic abundances, such as Barbuy (1985), Barbuy (1987), Barbuy et al. (1987), Gay & Lambert (2000), Yong et al. (2003a), Yong et al. (2003b), Yong et al. (2004), Meléndez & Cohen (2007), Meléndez & Cohen (2009) and Thygesen et al. (2016), but due to the difficulty in measuring the MgH lines we have little data, especially at low metallicities, to assess the evolution of the Mg isotopic ratios. Note that the MgH features are visible only in cool and not too evolved stars (Spinrad & Wood 1965). Regarding the halo population, a limited number of halo stars have been analyzed, with important contributions by Yong et al. (2003b) and Meléndez & Cohen (2007). Only seven single metal poor stars ($-2.60 <$ [Fe/H] < -1.35) from the Galactic halo have Mg isotopic measurements in the literature. Therefore, in this paper, we extended the metallicity range with our new sample and make it possible to assess when the ^{25,26}Mg abundances start to became important with respect to ^{24}Mg abundances to constrain the onset of AGB stars in the galactic halo, adding more insights to the galactic chemical evolution process.

The paper is organized as follows: in Sect. 2 we discuss how the three magnesium isotopes are formed; in Sect. 3, we show the sample and the stellar parameters; in Sect. 4, we describe the analysis, Sect. 5 shows the results and discussion and the conclusions are presented in Sect. 6.

2. PRODUCTION OF MAGNESIUM ISOTOPES IN DIFFERENT STELLAR SITES

The main magnesium isotope ^{24}Mg is produced inside massive stars during core carbon and neon burning before the supernova explosion. During core carbon burning, one of the most important reactions is ^{12}C(^{12}C, p)^{23}Na, where the product ^{23}Na is destroyed through the reaction ^{23}Na(p, γ)^{24}Mg which is responsible for the creation of ^{24}Mg. According to Arnett & Thielemann (1985), ^{24}Mg is the third most important product of core carbon burning in massive stars. During core neon burning, ^{20}Ne(γ, α)^{16}O is the main reaction (Thielemann & Arnett 1985) which generates $\alpha-$particles. These $\alpha-$particles, along with the remaining ^{20}Ne, form ^{24}Mg through the reaction ^{20}Ne(α, γ)^{24}Mg.

The isotopes ^{25,26}Mg are also produced in smaller amounts in massive stars in their outer carbon layers during helium burning (Woosley & Weaver 1995) through the reactions ^{22}Ne(α, n)^{25}Mg, ^{22}Ne(α, γ)^{26}Mg and ^{25}Mg(n, γ)^{26}Mg. For details on the amount of ^{24,25,26}Mg produced in massive stars, see Heger & Woosley (2010).

The magnesium isotopes are additionally produced in AGB stars. They can be formed in three possible regions: the hydrogen burning shell, the helium burning shell, and at the base of the convective envelope in intermediate-mass stars during hot bottom burning (for a review of AGB evolution, see Karakas & Lattanzio 2014).

The most important production site of ^{25,26}Mg is the helium burning shell in AGB stars (Karakas & Lattanzio 2003). During a thermal pulse, ^{22}Ne is created via successive α-captures onto ^{14}N. When the temperature of this region increases above $\approx 300 \times 10^6$ K, the stars experience an increase in ^{25,26}Mg through the reactions ^{22}Ne(α, n)^{25}Mg and ^{22}Ne(α, γ)^{26}Mg. Additionally, ^{26}Mg may also be produced by neutron capture via ^{25}Mg(n, γ)^{26}Mg.

During hot bottom burning in massive AGB stars, hydrogen burning occurs via the CNO cycle, Ne – Na and Mg – Al chains when the temperature is higher than 50×10^6 K. The lower densities at the base of the envelope mean that hydrogen burning reactions need to occur at higher temperatures than described in, e.g., Arnould et al. (1999). Thus, this site becomes important for the production and depletion of the magnesium isotopes (see Karakas & Lattanzio 2003 and Ventura & D'Antona 2011).

Magnesium isotopes are created via the Mg – Al chain (for details, see Arnould et al. 1999 or Karakas & Lattanzio 2003), but in the same chain they can also be destroyed. The isotope ^{25}Mg is destroyed through the reaction ^{25}Mg(p, γ)^{26}Al. The isotope ^{26}Mg experiences a little decrement through the reaction ^{26}Mg(p, γ)^{27}Al until temperatures of $\approx 60 \times 10^6$ K, but also experiences an abundance enhancement due to the decay of ^{26}Al in the hydrogen shell ashes. The abundance of ^{24}Mg remains almost stable at temperatures below about 70×10^6 K in the hydrogen burning shell, but in the most massive AGB stars the temperature at the base of the envelope may exceed 90×10^6 K, hot enough for the destruction of ^{24}Mg by proton capture.

Altogether, AGB stars are responsible for a considerable amount of ^{25,26}Mg isotopes produced in the Galaxy. Since the lifetime of a star depends on its mass and metallicity, the study of Mg abundances in Galactic halo main-sequence stars, which do not have their chemical composition affected by stellar evolution, can determine the onset of the effects of AGB evolution in the Galactic halo, and this can provide us insights on the timescale for formation of the Galactic halo.

3. SPECTRA AND STELLAR PARAMETERS

The sample consists of eight K dwarf stars from the galactic halo. These objects were chosen from the updated catalog of Ramírez & Meléndez (2005), where we considered the temperature interval (4000-5000 K) as well as the metallicity range of $-2 < $ [Fe/H] < -0.8. We discard binary stars to avoid contamination from the companion.

In order to get precise measurements for the three Mg isotopes, we need high resolution and good signal-to-noise spectra (> 150). These conditions were achieved thanks to the HIRES spectrograph (Vogt et al. 1994) at the Keck Observatory ($R \approx 10^5$ and $200 \leq$ S/N ≤ 300) in 2007 September. The spectral orders were extracted with MAKEE[1]. For Doppler correction, combining spectra, and continuum normalization, we used IRAF[2].

After the data reduction, we found that there were two double-lined stars in our sample, BD -004470 and G 3-13, which were discarded from the analysis. For the remaining stars, the stellar effective temperatures were derived according to the photometric calibration from Casagrande et al. (2010), using the values of B, V, J, H, and Ks magnitudes compiled by Soubiran et al. (2016).

The [Fe/H] and microturbulence values were determined by measuring Fe I and Fe II lines with the aid of IRAF and using the 2014 July version of the 1D LTE code MOOG (Sneden 1973). The Fe I and Fe II line list specifically for metal poor K dwarfs was taken from the

---

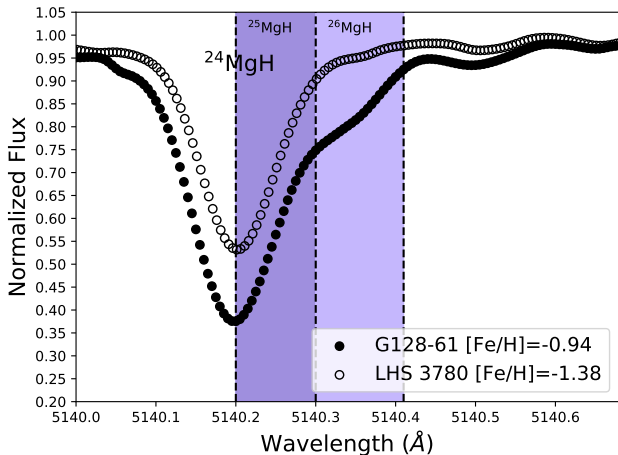[1] MAKEE was developed by T. A. Barlow specifically for reduction of Keck HIRES data. It is freely available at http://www.astro.caltech.edu/~tb/makee/.

[2] http://iraf.noao.edu/.

Figure 1. Spectra from stars with different [Fe/H] in the region 5140.2 Å of the MgH molecular feature.

work of Chen & Zhao (2006). The T_{eff} values derived here are compatible with previous works in the literature. We adopted literature values of surface gravity (log g) (Ramírez & Meléndez 2005; Yong & Lambert 2003). The stellar parameters are presented in Table 1.

As a result of the abundance analysis, we found a star with chemical anomalies, named LHS 173. The analysis of that star will be presented elsewhere.

4. ANALYSIS

Since the isotopes ^{25,26}Mg have a weak contribution in the wings of a stronger ^{24}MgH line, creating a red asymmetry in the MgH feature, we have to employ spectral synthesis to derive the Mg isotopic abundances.

As we can see in Fig. 1, for stars with similar temperatures but different [Fe/H], we have different amounts of MgH. The more metal poor the star is, the less MgH will be present. Furthermore, we can see that the red asymmetry is stronger in the more metal-rich star, suggesting a higher fraction of ^{25,26}Mg.

We determined the macroturbulence velocity broadening by analyzing the line profiles of the Fe I 6056.0 Å, 6078.5 Å, 6096.7 Å and 6151.6 Å lines, setting the rotational velocity broadening as zero. We also included the instrumental broadening in the calculations.

As recommended by McWilliam & Lambert (1988) and Gay & Lambert (2000), and also used in the works of Barbuy (1985, 1987), Yong et al. (2003b), Meléndez & Cohen (2007) and Meléndez & Cohen (2009), we adopted three wavelength regions to determine the Mg isotopic abundances ratios, namely 5134.6 Å, 5138.7 Å and 5140.2 Å.

The isotopic abundances are estimated as described in Meléndez & Cohen (2007), also using the code MOOG

and the Kurucz grid of ATLAS9 model atmospheres (Castelli & Kurucz 2004). The line list adopted in this region is the same used in the work of Meléndez & Cohen (2007), which includes both molecular and atomic lines. Although the abundance analysis was derived with 1D models, Thygesen et al. (2016, 2017) showed that using 3D models in the analysis of Mg isotopes does not have a significant impact, especially for ^{26}Mg/Mg.

The isotopic abundances are measured by performing a χ^2 fit, where $\chi^2 = \Sigma(O_i - S_i)/\sigma^2$, with O_i and S_i being the observed and synthetic spectra and $\sigma = (S/N)^{-1}$. A comparison of spectral synthesis and observed spectra is shown in the left panel of Fig. 2. The right panel of the Fig. 2 displays the variations of the χ^2 fits.

The final isotopic values, as well as the parameters adopted in the spectral synthesis, are presented in Table 1. The ^{25,26}Mg errors are the standard deviation between the isotopic ratios of the three regions adopted in this work. The line-to-line scatter in the isotopic percentages is only about 1%, showing the consistency among the different MgH features and the high precision achieved in this work.

5. DISCUSSION

The results including the current analysis plus data from the literature are shown in Fig. 3, note that the star LHS 3780 from the sample of Yong et al. (2003b) is not shown here since we present new isotopic abundances for this star in this work. The ^{25}Mg/Mg ratios should not be used to compare with Galactic chemical evolution models due to both observational uncertainties arising from the smaller isotopic shift in comparison with ^{24}Mg and to modeling uncertainties (i.e., the effects of 3D hydrodynamical model atmospheres shown in Thygesen et al. 2016, 2017). However, the ^{26}Mg/Mg ratio is robust, as the ^{26}Mg determination is almost immune to the effects of 3D hydrodynamical model atmospheres, as discussed in Thygesen et al. (2016, 2017).

We see that our data are consistent with previous measurements in the literature and with the model of Fenner et al. (2003), which does not include AGB stars, and Kobayashi et al. (2011), which includes the contribution from AGB stars, for halo dwarfs with [Fe/H] < −1.4. However, the model of Fenner et al. (2003) including the AGB contribution, does not match with the observational data.

It is possible to see as well that for stars with [Fe/H] > −1.4, the data differ somewhat (1-3 σ) from either of the models (Fenner et al. 2003 without AGB stars, and Kobayashi et al. 2011 including AGB stars). This suggests higher yields of the neutron-rich isotopes, in contrast to current yield predictions, or perhaps a dif-
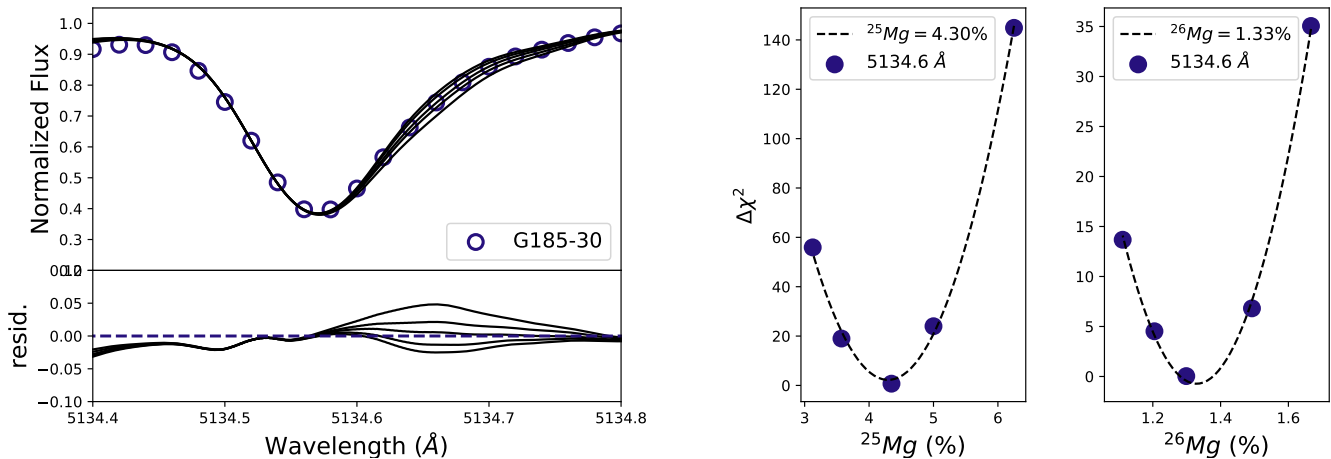
Figure 2. Left panel shows the MgH 5134.6 Å region with the observed spectrum (blue open circles) and the respective spectral synthesis for five different values represented by black solid lines. The right panel shows the χ^2 analysis with the best value of ^{25}Mg and ^{26}Mg. Both panels are for the star G 185-30.

Table 1. Stellar parameters and magnesium isotopic ratios.

Object	$T_{\text{eff.}}$ (K)	[Fe/H]	log g (dex)	$v_{\text{mic.}}$ (km s^{-1})	^{25}Mg (%)	^{26}Mg (%)
G 185-30	4524	-1.85±0.01	4.5[a]	0.00	4.0±0.3	1.6±0.4
G 128-61	4664	-0.94±0.02	5.0[b]	0.00	8.0±1.0	4.8±1.6
G 78-26	4288	-1.20±0.02	4.7[b]	0.24	5.3±0.2	3.4±0.6
G 189-45	4937	-1.33±0.01	4.3[b]	0.00	4.6±1.1	2.2±0.9
LHS 3780	4880	-1.38±0.01	4.5[b]	0.00	4.5±0.1	0.0±1.0
Sun	5777	0.00	4.44	1.00	10.00[c]	11.01[c]

Notes. [*]Magnesium isotopic ratios are given with respect to ^{24}Mg + ^{25}Mg + ^{26}Mg.

References. [a]Ramírez & Meléndez (2005). [b]Yong & Lambert (2003). [c]Asplund et al. (2009).

ferent value for the timescale formation of the halo (see below).

We adjusted a break function (Fig. 3, green dotted line in the right panel), including the data from the current work and values from the literature, in order to estimate a reliable metallicity at which low-metallicity AGB stars begin to contribute to galactic chemical enrichment. The metallicity achieved with this work ([Fe/H]= −1.4±0.1) is slightly higher than the one determined by the study of Meléndez & Cohen (2007). According to our results, AGB stars begin to contribute to the Mg isotopes at a metallicity of [Fe/H] > −1.4. In order to compare our contribution with a new sample of stars relative to the previous data in the literature, we also adjusted a break function considering only the data from literature (Fig. 3, red dotted line in the right panel). Thus, we conclude that our new data is essen-

tial to better establish the break point when ^{26}Mg/Mg starts to rise.

The study of Shingles et al. (2015) suggests that for [Fe/H] = -1.4 the majority of the contribution comes from AGB stars with $\gtrsim 4 \pm 1$ solar masses (Fig. 4). For stars in this mass interval, the lifetime is between approximately $\lesssim 150 - 300$ million of years. Thus, if we were just to consider AGB stars, we would suggest a short timescale for the formation of the galactic halo.

However, if we simply set a short duration of star formation for the halo, it is not possible to reproduce our observed ^{26}Mg/Mg ratios at [Fe/H] > −1.4. This is because core-collapse supernovae produce ^{24}Mg at the same time when AGB stars produce ^{26}Mg. It is necessary to suppress the contribution from core-collapse supernovae and to make the AGB contribution dominant for the chemical enrichment in the halo. One way to model this is to introduce a strong outflow. In Fig. 5,
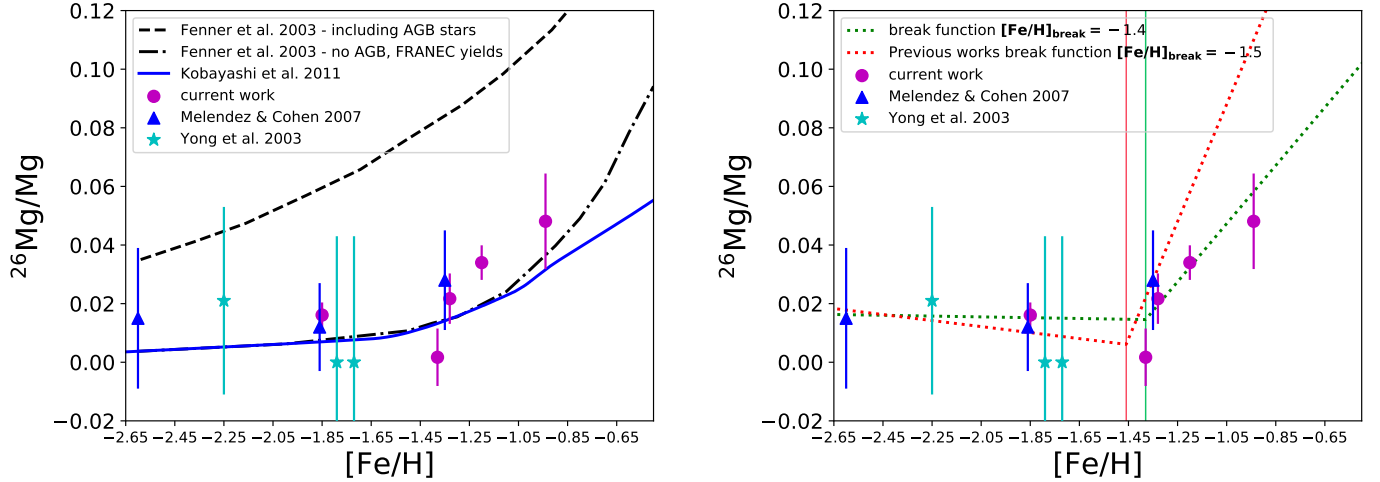
Figure 3. In both panels, purple circles represent the data determined in this work, blue triangles show the data from Meléndez & Cohen (2007) and the cyan stars exhibit results from Yong et al. (2003b). In the left panel, the black dotted-dashed line shows a model from Fenner et al. (2003) with no AGB contribution, the black dashed line shows a model from the same work with AGB contribution and the model for the solar neighborhood from Kobayashi et al. (2011) is represented by the blue solid line. The green dotted line in the right panel shows the break function considering all the observed data and the red dotted line shows the break function considering only the data from Yong et al. (2003b) and Meléndez & Cohen (2007), the red and green vertical lines indicate [Fe/H]= −1.5 and [Fe/H]= −1.4 respectively.
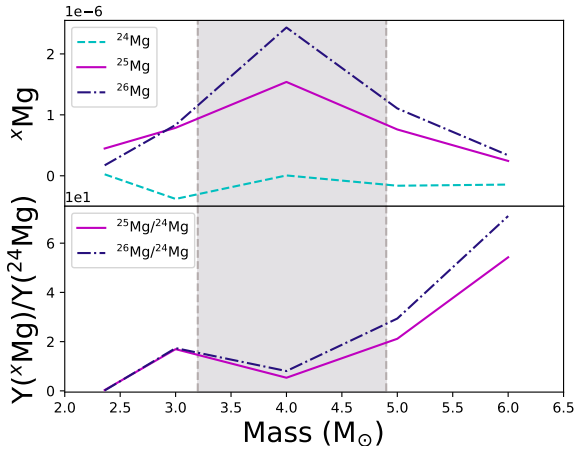

Figure 4. Top: AGB stellar yields from Shingles et al. (2015) weighted by the initial mass function of Kroupa et al. (1993). Bottom: mass isotopic ratios for the same data. The gray area indicates the region where we have the majority contribution of ^{25,26}Mg isotopes. Data are from Shingles et al. (2015).

a new galactic evolution model (dotted-dashed line) considering this strong gas outflow for the halo is presented and compared to our data. In this new model, the chemical evolution in a system (i.e., Galactic halo) is numerically computed with the basic equations in Kobayashi et al. 2000 (Equations 5 and 6) and the outflow term in Kobayashi et al. 2006 (page 1165). The SFR is proportional to the gas fraction; $\phi = (1/\tau_s)f_g$. The driving

source of the outflow is the feedback from supernovae, and hence the outflow rate is also proportional to the gas fraction; $R_{out} = (1/\tau_o)f_g$. The initial gas fraction is set to be $f_g(0) = 1$ with no metallicity. The new stars are formed from the mix of the remaining primordial gas plus any gas ejection of previous generations of stars (i.e., mass loss and supernovae). The outflow also removes some metals with the composition of the average metallicity of the system at the time, $R_{out}Z(t)$. The outflow gas could later fall onto the disk, but this process is not included in the model. Since this is not a dynamical model, the timescales are determined to reproduce observations, namely, the observed metallicity distribution function (Chiba & Yoshii 1998, see also Kobayashi et al. 2011 for a more detailed discussion). It is possible to have inflow as well, but the timescale should be short. Otherwise, it is not possible to reproduce the low metallicity of the Galactic halo stars.

In the best-fit model, the star formation and outflow timescales are $\tau_s = 5$ and $\tau_o = 0.2$ Gyr, respectively, with no inflow. The Kroupa IMF is adopted. Note that super-AGB yields are also included in this model, but the contribution is negligible (C. Kobayashi et al. 2018, in preparation). Other parameter sets are also possible such as $\tau_s = 10$ and $\tau_o = 0.4$ Gyr, but the outflow timescale should be no longer than $\tau_o = 0.4$ Gyr to explain our data at [Fe/H]= −0.94. Half of the halo stars are likely to be formed within 0.7 Gyr for $\tau_o = 0.2$ Gyr or should be formed within 1.5 Gyr for $\tau_o = 0.4$
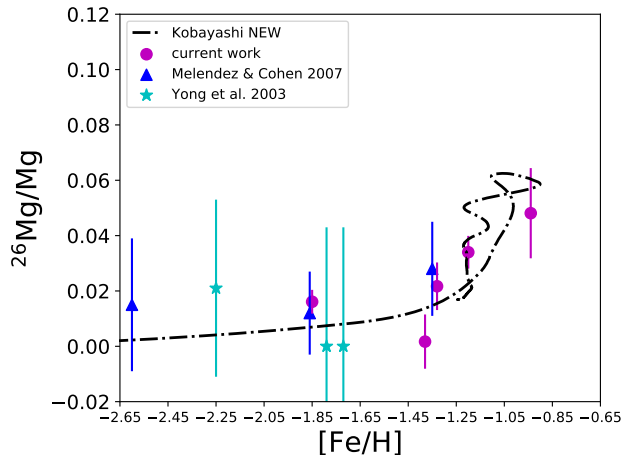
Figure 5. Our new model based upon Kobayashi et al. (2011), but now considering strong outflow. The observed data (see Fig. 3) are also plotted for comparison.

Gyr. With these short outflow timescale, the outflow gas contains the metals mostly produced by supernovae, while the new stars contain the metals mostly ejected from AGB stars. In the original halo model in Kobayashi et al. (2011) with $\tau_s = 15$ and $\tau_o = 1$ Gyr, only 15% of halo stars are formed within 1.5 Gyr, and this model does not show the rapid increase of $^{26}Mg/Mg$ ratios, very similar to the solar neighborhood model in Fig. 3 (solid line). From the various constraints, we suggest that the timescale for the formation of the halo should be below 1.5 Gyr.

Although we used a one-zone chemical evolution model for comparison with the observed data, we can stress that our short timescales of inflow and outflow suggest that the potential of the star forming region is likely shallow, and the progenitor system could be satellite galaxies, which is consistent with hydrodynamical simulations such as in Monachesi et al. (2016).

6. CONCLUSIONS

Due to high resolution and excellent signal-to-noise spectra obtained with HIRES at the 10 m Keck I telescope, we were able to determine the magnesium isotopic abundances with very high precision for five stars, thus

almost doubling the data from the literature of single metal poor halo dwarfs.

Here we stress that our conclusions are made with the addition of only two more stars at the high metallicity end, adding more is difficult due to observational limitations. It is with this additional data that it is now possible to better estimate when the contribution from AGB stars became important for the galactic halo. From this work, we can confirm that ^{26}Mg abundances start to rise for stars with $[Fe/H] > -1.4$.

We conclude that for $[Fe/H] > -1.4$ the Mg isotope ratios somewhat disagree with previous chemical evolution model predictions, indicating higher yields of the neutron-rich isotopes, in contrast to current yield predictions. However, the disagreement between the data and the models can also be explained with a different formation timescale of the galactic halo.

According to calculations available in the literature, for $[Fe/H] > -1.4$ the majority of contribution on the heaviest Mg isotopes comes from AGB stars with masses of about $4\pm1M_\odot$, which have a lifetime between of about 150-300 million years, which indicates a very short formation timescale of the galactic halo. We present a new halo model that reproduces the rapid increase of $^{26}Mg/Mg$ ratios, by including a strong outflow. From the parameter study of the chemical evolution models, we conclude that the upper limit for the formation timescale is 1.5 Gyr.

REFERENCES

Alibés, A., Labay, J., & Canal, R. 2001, Astronomy & Astrophysics, 370, 1103

Arnett, W. D., & Thielemann, F.-K. 1985, ApJ, 295, 589

Arnould, M., Goriely, S., & Jorissen, A. 1999, A&A, 347, 572

Asplund, M., Grevesse, N., Sauval, A. J., & Scott, P. 2009, ARA&A, 47, 481

Barbuy, B. 1985, A&A, 151, 189

—. 1987, A&A, 172, 251

Barbuy, B., Spite, F., & Spite, M. 1987, A&A, 178, 199

Carollo, D., Beers, T. C., Lee, Y. S., et al. 2007, Nature, 450, 1020

Casagrande, L., Ramírez, I., Meléndez, J., Bessell, M., & Asplund, M. 2010, A&A, 512, A54

Castelli, F., & Kurucz, R. L. 2004, ArXiv Astrophysics e-prints, astro-ph/0405087

Chen, Y. Q., & Zhao, G. 2006, MNRAS, 370, 2091

Chiappini, C., Matteucci, F., & Gratton, R. 1997, ApJ, 477, 765

Chiba, M., & Yoshii, Y. 1998, AJ, 115, 168

Eggen, O. J., Lynden-Bell, D., & Sandage, A. R. 1962, ApJ, 136, 748

Fenner, Y., Gibson, B. K., Lee, H.-c., et al. 2003, PASA, 20, 340

Fishlock, C. K., Karakas, A. I., Lugaro, M., & Yong, D. 2014, ApJ, 797, 44

Gay, P. L., & Lambert, D. L. 2000, ApJ, 533, 260

Heger, A., & Woosley, S. E. 2010, ApJ, 724, 341

Hunter, J. D. 2007, Computing In Science & Engineering, 9, 90

Karakas, A. I., & Lattanzio, J. C. 2003, PASA, 20, 279

—. 2014, PASA, 31, e030

Kobayashi, C., Karakas, A. I., & Umeda, H. 2011, MNRAS, 414, 3231

Kobayashi, C., & Nakasato, N. 2011, ApJ, 729, 16

Kobayashi, C., Tsujimoto, T., & Nomoto, K. 2000, ApJ, 539, 26

Kobayashi, C., Umeda, H., Nomoto, K., Tominaga, N., & Ohkubo, T. 2006, ApJ, 653, 1145

Kroupa, P., Tout, C. A., & Gilmore, G. 1993, MNRAS, 262, 545

McWilliam, A., & Lambert, D. L. 1988, MNRAS, 230, 573

Meléndez, J., & Cohen, J. G. 2007, ApJL, 659, L25

—. 2009, ApJ, 699, 2017

Micali, A., Matteucci, F., & Romano, D. 2013, MNRAS, 436, 1648

Monachesi, A., Gómez, F. A., Grand, R. J. J., et al. 2016, MNRAS, 459, L46

Navarro, J. F., Frenk, C. S., & White, S. D. M. 1997, ApJ, 490, 493

Nissen, P. E., & Schuster, W. J. 2010, A&A, 511, L10

Ramírez, I., & Meléndez, J. 2005, ApJ, 626, 446

Searle, L., & Zinn, R. 1978, ApJ, 225, 357

Shingles, L. J., Doherty, C. L., Karakas, A. I., et al. 2015, MNRAS, 452, 2804

Sneden, C. A. 1973, PhD thesis, THE UNIVERSITY OF TEXAS AT AUSTIN.

Soubiran, C., Le Campion, J.-F., Brouillet, N., & Chemin, L. 2016, A&A, 591, A118

Spinrad, H., & Wood, D. B. 1965, ApJ, 141, 109

Thielemann, F. K., & Arnett, W. D. 1985, ApJ, 295, 604

Thygesen, A. O., Kirby, E. N., Gallagher, A. J., et al. 2017, ApJ, 843, 144

Thygesen, A. O., Sbordone, L., Ludwig, H.-G., et al. 2016, A&A, 588, A66

Tissera, P. B., White, S. D. M., & Scannapieco, C. 2012, MNRAS, 420, 255

Tody, D. 1986, in Proc. SPIE, Vol. 627, Instrumentation in astronomy VI, ed. D. L. Crawford, 733

Tody, D. 1993, in Astronomical Society of the Pacific Conference Series, Vol. 52, Astronomical Data Analysis Software and Systems II, ed. R. J. Hanisch, R. J. V. Brissenden, & J. Barnes, 173

van der Walt, S., Colbert, S. C., & Varoquaux, G. 2011, Computing in Science & Engineering, 13, 22

Ventura, P., & D'Antona, F. 2011, MNRAS, 410, 2760

Vogt, S. S., Allen, S. L., Bigelow, B. C., et al. 1994, in SPIE Proceedings, Vol. 2198, Instrumentation in Astronomy VIII, ed. D. L. Crawford & E. R. Craine, 362

Woosley, S. E., & Weaver, T. A. 1995, ApJS, 101, 181

Yong, D., Grundahl, F., Lambert, D. L., Nissen, P. E., & Shetrone, M. D. 2003a, A&A, 402, 985

Yong, D., & Lambert, D. L. 2003, PASP, 115, 22

Yong, D., Lambert, D. L., Allende Prieto, C., & Paulson, D. B. 2004, ApJ, 603, 697

Yong, D., Lambert, D. L., & Ivans, I. I. 2003b, ApJ, 599, 1357

Zolotov, A., Willman, B., Brooks, A. M., et al. 2009, ApJ, 702, 1058